

# UNC-83 is a nuclear-specific cargo adaptor for kinesin-1-mediated nuclear migration

Marina Meyerzon, Heidi N. Fridolfsson, Nina Ly, Francis J. McNally and Daniel A. Starr\*

Intracellular nuclear migration is essential for many cellular events including fertilization, establishment of polarity, division and differentiation. How nuclei migrate is not understood at the molecular level. The *C. elegans* KASH protein UNC-83 is required for nuclear migration and localizes to the outer nuclear membrane. UNC-83 interacts with the inner nuclear membrane SUN protein UNC-84 and is proposed to connect the cytoskeleton to the nuclear lamina. Here, we show that UNC-83 also interacts with the kinesin-1 light chain KLC-2, as identified in a yeast two-hybrid screen and confirmed by in vitro assays. UNC-83 interacts with and recruits KLC-2 to the nuclear envelope in a heterologous tissue culture system. Additionally, analysis of mutant phenotypes demonstrated that both KLC-2 and the kinesin-1 heavy chain UNC-116 are required for nuclear migration. Finally, the requirement for UNC-83 in nuclear migration could be partially bypassed by expressing a synthetic outer nuclear membrane KLC-2::KASH fusion protein. Our data support a model in which UNC-83 plays a central role in nuclear migration by acting to bridge the nuclear envelope and as a kinesin-1 cargo-specific adaptor so that motor-generated forces specifically move the nucleus as a single unit.

**KEY WORDS:** Kinesin-1, Nuclear envelope, KASH proteins, SUN proteins, Nuclear migration, UNC-83

## INTRODUCTION

Understanding how the subcellular targeting of molecular motors is regulated is key to understanding their functions. Little is currently known about the mechanisms by which kinesin motors are recruited to specific cargos at specific times. Kinesin-1 is the founding member of the kinesin family of microtubule motors (Vale et al., 1985) and consists of two heavy chains that contain the motor and microtubule-binding sites and two light chains that provide cargo specificity and regulation. Kinesin-1 functions are best understood in the axons of motoneurons. Kinesin light chain is thought to regulate the cargo-binding specificity of the heavy chain, although in the transport of mitochondria in *Drosophila* axons and photoreceptor cells the adapter protein Milton functions to target the heavy chain to mitochondria independently of the light chain (Glater et al., 2006). Kinesin light chains are targeted to neuronal vesicles through JNK-interacting proteins (JIPs; JIP3 is SYD in *Drosophila* and UNC-16 in *C. elegans*) (Bowman et al., 2000). More-specific vesicular transmembrane proteins, such as ApoER2 (LRP8) and calyntenin 1, also contribute to cargo specificity (Konecna et al., 2006; Verhey et al., 2001).

Kinesin-1 has also been shown to play a role in the positioning of multiple cargos in non-neural cells, including mitochondria, vesicles, lysosomes, endoplasmic reticulum (ER), lipid droplets, mRNAs and meiotic spindles (Gindhart, 2006; Karcher et al., 2002). However, the mechanisms that target kinesin-1 to specific cargos outside of the axon are less well understood. For example, kinesin-1 interacts with kinectin to position the ER (Ong et al., 2000; Toyoshima et al., 1992). Additionally, kinesin-1 functions in conjunction with KCA-1 to position the *C. elegans* female meiotic spindle to the cortex (Yang et al., 2005) and has been proposed to function with Klarsicht to move lipid droplets in *Drosophila*

embryos (Guo et al., 2005; Shubeita et al., 2008; Welte et al., 1998). Kinesin-1 has also been hypothesized to function in nuclear migration in *C. elegans* hypodermal cells (Williams-Masson et al., 1998). The nucleus is possibly the largest kinesin cargo, but it remains unknown if or how kinesin-1 is targeted to the surface of the nucleus. Here we report that *C. elegans* UNC-83 is the outer nuclear envelope-specific kinesin-1 cargo adaptor.

Nuclear positioning is required for a number of cellular and developmental events in eukaryotes, including fertilization, establishment of polarity, cell division and differentiation (Starr, 2007). The *C. elegans* hyp7 embryonic hypodermal precursor cells provide an excellent model for the study of nuclear migration (Sulston, 1983; Williams-Masson et al., 1998). Mutations in *unc-83* or *unc-84* disrupt nuclear migration in hyp7 cells, larval hypodermal P-cells and in embryonic intestinal primordial cells (Horvitz and Sulston, 1980; Malone et al., 1999; Starr et al., 2001; Sulston and Horvitz, 1981). Failure of hyp7 precursor nuclear migration results in mispositioning of the nuclei to the dorsal cord of the newly hatched animal, whereas failure of P-cell nuclear migration leads to egg laying and uncoordinated phenotypes due to the death of epithelial and neuronal precursors (Horvitz and Sulston, 1980; Sulston and Horvitz, 1981).

UNC-84 and UNC-83 are novel transmembrane proteins with conserved Sad1p/UNC-84 (SUN) and Klarsicht/ANC-1/Syne homology (KASH) domains, respectively, at their C-termini (Malone et al., 1999; Starr and Fischer, 2005; Starr et al., 2001). UNC-83 and UNC-84 bridge the nuclear envelope and are hypothesized to connect the cytoskeleton to the nuclear lamina. In the nuclear envelope bridging model, UNC-84 localizes to the inner nuclear membrane, interacts with lamin and recruits UNC-83 to the outer nuclear membrane through a direct interaction between the SUN and KASH domains in the perinuclear space (McGee et al., 2006). In this model, the large N-terminal domain of UNC-83 resides on the cytoplasmic surface of the nucleus where it functions to regulate the forces required for nuclear migration. The structure of the cytoplasmic domain of UNC-83 is unknown and exhibits no sequence homology with other known proteins. Prior to this study, the mechanisms by which UNC-83

Department of Molecular and Cellular Biology, University of California, Davis, CA 95616, USA.

\*Author for correspondence (e-mail: dastarr@ucdavis.edu)

regulates or generates the forces to reposition nuclei were unknown. Here, we show that UNC-83 functions as a kinesin-1 docking site at the outer nuclear membrane.

## MATERIALS AND METHODS

### *C. elegans* strains and characterization

The N2 strain was used for wild type. The *unc-83(e1408)*, *klc-2(km28)*, *klc-2(km11)*, *unc-116(e2310)*, *unc-116(rh24sb79)* and *unc-116(f122)* alleles were previously described (Patel et al., 1993; Starr et al., 2001; Sakamoto et al., 2005; Yang et al., 2005) (D. Thierry-Mieg, personal communication). Some strains were provided by the Caenorhabditis Genetics Center, which is funded by the NIH National Center for Research Resources. Transgenic lines were created by standard DNA microinjection techniques, using either a *sur-5::gfp* construct or an *odr-1::rfp* construct as a transformation marker (Sagasti et al., 2001; Yochem et al., 1998). Dorsal cord nuclei were counted in L1 larvae using differential interference contrast (DIC) optics and a 63× PLAN APO 1.40 objective on a Leica DM 6000 compound microscope. Animals were only identified as transgenic or non-transgenic after counting.

### Yeast two-hybrid screen

Codons corresponding to amino acids 137-692 of UNC-83c were amplified by PCR and inserted into the bait vector pDEST32 via Gateway Technology (Invitrogen). The resulting UNC-83 bait plasmid (pSL320) was transformed into the yeast strain AH109 (Clontech). Controls were performed to ensure that the bait construct did not self-activate the *HIS3* and *lacZ* reporters. An Invitrogen mixed-stage *C. elegans* cDNA library (28 µg) was used to transform yeast carrying the UNC-83 bait plasmid and positives were selected on Leu<sup>-</sup> Trp<sup>-</sup> His<sup>-</sup> medium containing 50 mM 3-amino-1,2,4-triazole (Sigma-Aldrich). Approximately  $1.4 \times 10^7$  clones were screened. The details of this screen will be published elsewhere. For directed yeast two-hybrid analysis, UNC-83c (137-362) and (137-692) were cloned into pDEST32 and into the GAL4 activation domain bait vector pDEST22 using Gateway Technology. KLC-2 (4-561), (4-122), (4-176) and (177-561) were cloned into pDEST32 and pDEST22 as above. Controls were performed to ensure that none of the baits self-activated the reporters. Activation of the *HIS3* reporter was assayed by growth on Leu<sup>-</sup> Trp<sup>-</sup> His<sup>-</sup> medium supplemented with 3-amino-1,2,4-triazole at 10-50 mM, depending on the bait used. Activation of the *lacZ* reporter was tested by filter-lift β-galactosidase assay.

### In vitro and in vivo protein interaction assays

UNC-83c (1-698) and (137-362) were amplified by PCR from the EST yk230e1 (Starr et al., 2001) and cloned into pMAL-c2X (New England Biolabs) to create MBP-UNC-83 constructs pDS31 and pSL407, respectively (Starr et al., 2001). KLC-2 (1-561) was amplified by PCR from a two-hybrid positive and cloned into pGEX-2T (GE Biosciences) to create the GST-KLC-2 construct pSL409. pMAL-c2X and pGEX-2T were used alone to express MBP (maltose binding protein) or GST (glutathione-S-transferase). Fusion proteins were expressed in *E. coli* strain BL21-CodonPlus (Stratagene) and purified on glutathione (GE Biosciences) or amylose (New England Biolabs) columns. An excess of purified MBP or MBP-UNC-83 was added along with crude *E. coli* strain OP50 extract (10 mg/ml) in PBS containing 10% glycerol to the GST or GST::KLC-2-bound beads. Binding reactions were incubated for 2 hours at 4°C. After washing five times, bound protein was analyzed by SDS-PAGE and Coomassie Blue staining.

UNC-83cΔKASH (1-698) and UNC-83c full-length were cloned into pCS2+MT (Rupp et al., 1994) to create pSL446 and 451, respectively. KLC-2 was cloned into pEGFP-c3 (BD Biosciences) to create pSL450. HeLa cells were transiently transfected using 6 µl of Lipofectamine (Invitrogen) and 0.5 µg of each plasmid DNA per ml of media. Extracts were prepared as described by Yang et al. (Yang et al., 1999) and incubated with 2 µl anti-KLC-2 antibodies per ml of extract (Yang et al., 2005); the KLC-2 complex was purified on protein A beads (GE Life Sciences).

### Immunofluorescence and immunoblots

*C. elegans* embryos were stained as described by Starr et al. (Starr et al., 2001). HeLa cells were transfected and stained as described by McGee et al. (McGee et al., 2006). The UNC-83 mouse monoclonal antibody 1209D7D5

(Starr et al., 2001) was used undiluted. The KLC-2 and UNC-116 rabbit polyclonal antibodies (Yang et al., 2005) were used at 1/1000 dilution. The mouse monoclonal 9E10 anti-myc antibody (Developmental Studies Hybridoma Bank, University of Iowa) was used at 1/500. Rabbit polyclonal antibody NB600-308 against GFP (Novus Biologicals) was used at 1/500. Cy2-conjugated goat anti-mouse IgG and Cy3- or Cy2-conjugated goat anti-rabbit IgG (Jackson ImmunoResearch) were used as secondary antibodies at 1/200. DNA was visualized with DAPI.

For immunoblot analysis, wild-type and mutant animals were grown to near starvation, collected from plates and washed in M9 buffer and water, and subsequently boiled in an equal volume of 2×SDS dye. The worm lysates were separated on a 7% polyacrylamide gel and blotted onto nitrocellulose. Proteins were visualized using the KLC-2 and UNC-116 rabbit polyclonal antibodies (Yang et al., 2005) at 1/10,000 or the rabbit anti-GFP antibody at 1/5000. Goat anti-rabbit HRP (Jackson ImmunoResearch) was used as secondary antibody at 1/10,000.

Images were collected using a Leica DM 6000 with a 63× PLAN APO 1.40 objective, a Leica DC350 FX camera and Leica FW4000 software. Confocal images were collected using an Olympus FV1000 laser-scanning confocal microscope. Images were uniformly enhanced using the level and contrast commands in Adobe Photoshop.

### KLC-2::KASH construct

To create the KLC-2::myc::KASH construct, a 6.5 kb *XhoI*-*BamHI* fragment of WRM0616aH11, which rescues hyp7 nuclear migration in *klc-2(km28)* mutants, was cloned into pBlueScript (pBS) (Stratagene). The 6-myc-tag-encoding *BamHI*-*XhoI* fragment of pCS2+MT was cloned into the pBS/KLC-2 construct downstream of KLC-2. A 2.3 kb fragment of pDS22 (Starr et al., 2001) containing the transmembrane and KASH domains of UNC-83, as well as the 3' UTR, was amplified by PCR using appropriate overhanging restriction sites and cloned into the *NorI* site of the pBS/KLC-2-6myc plasmid to create pSL440.

## RESULTS

### The kinesin-1 light chain interacts with the cytoplasmic domain of UNC-83

To identify proteins that interact with the cytoplasmic domain of UNC-83, a yeast two-hybrid screen of a *C. elegans* mixed-stage cDNA library was conducted. Amino acids 137-692 of UNC-83c were used as the bait. The bait construct began just after a series of aspartic acid residues, which would have been likely to cause the full-length UNC-83 construct to self-activate the *HIS3* reporter, and ends just before the transmembrane and KASH domains. Approximately  $1.4 \times 10^7$  clones were screened and 45 unique potential interacting partners of UNC-83 were identified (our unpublished data). One of these clones was isolated from the screen 20 times (by far the most frequent hit) and found to encode KLC-2. The UNC-83–KLC-2 interaction was confirmed in a directed yeast two-hybrid analysis using amino acids 4-561 of KLC-2 as bait and amino acids 137-692 of UNC-83c as prey (our unpublished data). *C. elegans klc-2* encodes a kinesin light chain, which interacts with the kinesin heavy chain protein UNC-116 to form the kinesin-1 complex (Sakamoto et al., 2005). KLC-2 has been shown to function in the localization of synaptic vesicles, in axonal outgrowth and in the translocation of the meiotic spindle to the oocyte cortex (Sakamoto et al., 2005; Tsuboi et al., 2005; Yang et al., 2005).

KLC-2 is thought to function as a cargo adaptor for kinesin-1. Most of the proteins known to interact with kinesin light chain bind to the run of six tetratricopeptide repeats (TPRs) in the C-terminal half of KLC-2 (Bowman et al., 2000; Konecna et al., 2006; Sakamoto et al., 2005; Verhey et al., 2001). However, one kinesin-1 cargo, the GSK3-binding protein (GBP/Frat), binds to the N-terminal region of the kinesin light chain at the same time as the

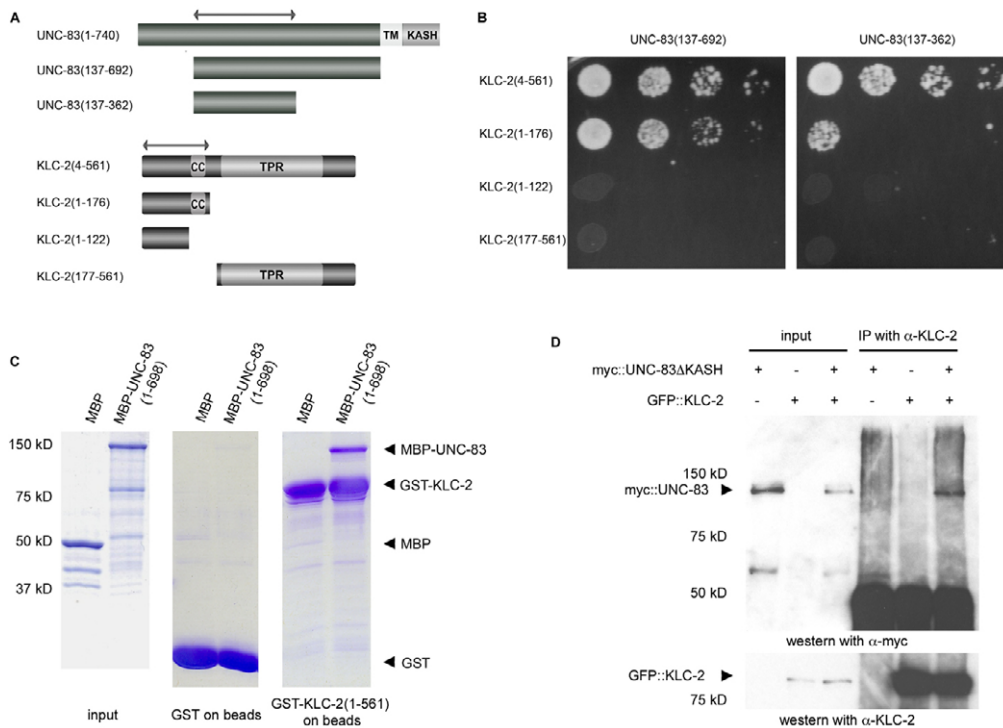


**Fig. 1. UNC-83 interacts with KLC-2.** (A) Constructs of *C. elegans* UNC-83 and KLC-2 used for yeast two-hybrid and GST in vitro interaction analysis. The cytoplasmic portion of UNC-83 is dark gray. The transmembrane (TM) and KASH domains of UNC-83 and the coiled-coil (CC) and tetratricopeptide repeat (TPR) domains of KLC-2 are indicated. Double-headed arrows indicate the KLC-2-binding domain of UNC-83 and the UNC-83-binding domain of KLC-2. (B) Yeast two-hybrid interactions between UNC-83c (137-362) or UNC-83c (137-692) as bait and the indicated regions of KLC-2 as prey. Serial dilutions of log-phase cultures are shown. (C) Coomassie Blue stained SDS-PAGE gels demonstrating the interactions between GST-KLC-2 (1-561) and MBP-UNC-83 (1-698). In the left-hand panel, 1% of the input proteins are shown. The middle panel shows the amount of proteins pulled down by beads with GST only, to show background. The right-hand panel shows MBP and MBP-UNC-83 fusion proteins pulled down by GST-KLC-2 beads. Arrowheads mark the expected positions of the indicated constructs. (D) myc::UNC-83ΔKASH was co-immunoprecipitated with anti-KLC-2 antibodies. A western blot probed with anti-myc antibodies to recognize myc::UNC-83ΔKASH is shown in the top panel. Lanes 1-3 show transfected HeLa cell extracts used as inputs. Lanes 4-6 show immunoprecipitation by anti-KLC-2 antibodies from the same extracts. Beneath is shown the same blot probed with anti-KLC-2 antibodies. Size standards and the UNC-83 and KLC-2 fusion proteins are indicated on the left.

heavy chain (Weaver et al., 2003). Yeast two-hybrid assays were performed to identify the domains of UNC-83 and KLC-2 required for binding to one another (Fig. 1A,B). Amino acids 137-362 of UNC-83c were sufficient to bind to nearly full-length KLC-2a (4-561) (Fig. 1B). An N-terminal construct of KLC-2 (4-176) was also able to bind to UNC-83, indicating that the TPR repeats are not necessary for the interaction with UNC-83 (Fig. 1B). KLC-2 truncated before the coiled-coil domain (4-122) was no longer able to bind to UNC-83, suggesting that at least some of residues 122-176, which include the coiled-coil domain, are required for this interaction (Fig. 1B). Thus, UNC-83 binds the N-terminal region of KLC-2 that contains the coiled-coil domain but not the TPR domain.

To confirm the two-hybrid interaction between UNC-83 and KLC-2, in vitro GST pull-down experiments were performed (Fig. 1C). GST::KLC-2 fusion proteins expressed in *E. coli* and purified onto glutathione beads were used to purify MBP::UNC-83 fusion proteins. Full-length GST::KLC-2 was able to bind to full-length MBP::UNC-83. To further confirm these in vitro pull-down results, UNC-83 and KLC-2 were co-expressed in a heterologous mammalian tissue culture system. HeLa cells were transfected with plasmids encoding a myc-tagged version of the cytoplasmic domain of UNC-83c and GFP-tagged KLC-2.

Immunoprecipitation with the anti-KLC-2 antibody pulled down myc-UNC-83ΔKASH (Fig. 1D). Therefore, based on yeast two-hybrid, in vitro GST pull-down and in vivo co-immunoprecipitation experiments, we conclude that UNC-83 directly interacts with KLC-2.

### Kinesin-1 is required for nuclear migration

To test whether kinesin-1 has similar functions to UNC-83, *klc-2* and *unc-116* mutants were analyzed for nuclear migration defects in *hyp7* precursor cells. In wild-type animals, *hyp7* nuclei migrate across the length of the cells (Sulston, 1983), whereas in *unc-83(e1408)* null animals nuclear migration is disrupted and *hyp7* nuclei are mislocalized to the dorsal cord of L1 larvae (Horvitz and Sulston, 1980; Sulston and Horvitz, 1981) (Fig. 2A-C). In *unc-83(e1408)* mutants,  $11.8 \pm 0.14$  (average  $\pm$  s.e.m.) nuclei were observed in the dorsal cord ( $n=71$ ), as compared with  $0 \pm 0$  in the wild type ( $n=30$ ). To examine the in vivo role of *klc-2* during nuclear migration, we analyzed *hyp7* nuclear migration in two *klc-2* mutant lines. The *klc-2(km28)* allele is a 0.6 kb deletion of the gene, which includes the region that encodes the coiled-coil domain (Sakamoto et al., 2005). This mutant line undergoes L1 larval arrest owing to defects in axonal transport and *klc-2(km28)* is likely to be a null allele (Sakamoto et al., 2005). The *klc-*

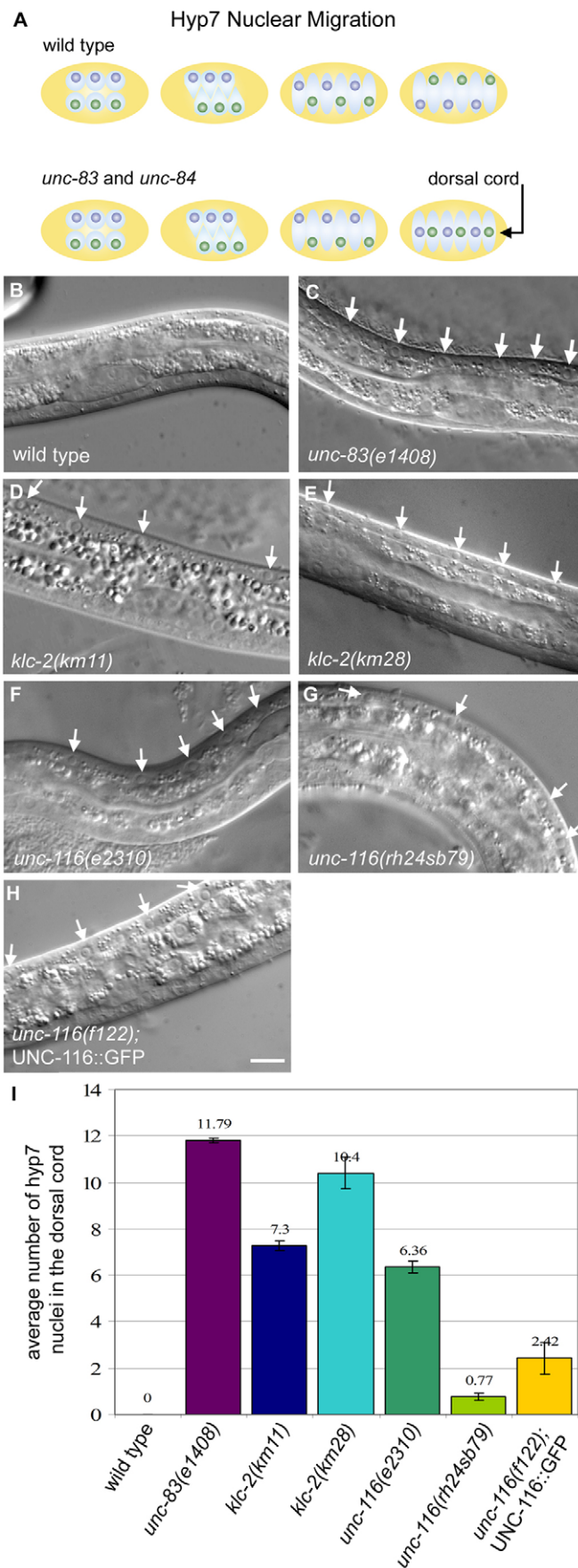


**Fig. 2. Loss-of-function alleles of *klc-2* or *unc-116* cause defects in hyp7 nuclear migration.** (A) Dorsal view of a pre-comma stage *C. elegans* embryo illustrating intercalation and nuclear migration of hyp7 precursors in wild-type and *unc-83* or *unc-84* embryos. The embryo is depicted in yellow. The cytoplasm of the hyp7 precursors is light blue, nuclei that migrate from right to left are dark blue, and nuclei that migrate from left to right are green. Anterior is on the left, right is up. (B–H) Lateral view of L1 hermaphrodites; dorsal is up. (B) Wild type. (C) *unc-83(e1408)*. (D) *klc-2(km11)*. (E) *klc-2(km28)*. (F) *unc-116(e2310)*. (G) *unc-116(rh24sb79)*. (H) *unc-116(f122); UNC-116::GFP*. White arrows mark hyp7 nuclei in the dorsal cord. Scale bar: 10  $\mu$ m. (I) The average number of hyp7 nuclei counted in the dorsal cord. Numbers above bars indicate averages; error bars indicate s.e.

*2(km11)* mutant is a partial loss-of-function mutation that results in viable, slightly uncoordinated (Unc) animals. This mutation is a 1.4 kb deletion of the gene, but the *klc-2(km11)* mutant also carries a second copy of the *klc-2* gene, inserted upstream of the endogenous locus (Sakamoto et al., 2005). These mutants were examined for hyp7 nuclear migration defects by counting the number of nuclei in the dorsal cords of L1 animals. *klc-2(km11)* had  $7.3 \pm 0.23$  nuclei in the dorsal cord (Fig. 2D,I;  $n=46$ ), indicating defects in hyp7 nuclear migration. We were able to count hyp7 nuclei in rare escaper *klc-2(km28)* mutant worms that had survived long enough into the L1 stage for their nuclei to be clearly seen; these mutants showed an average of  $10.4 \pm 0.73$  nuclei in their dorsal cords (Fig. 2E,I;  $n=9$ ). Thus, loss of function in *klc-2* negatively affects hyp7 nuclear migration.

KLC-2 interacts with UNC-116 to form the kinesin-1 complex in *C. elegans* (Sakamoto et al., 2005). To determine whether UNC-116 also functions in hyp7 nuclear migration, we counted the number of nuclei in the dorsal cords of animals from three *unc-116* mutant strains. *unc-116(e2310)*, a viable, weak loss-of-function allele caused by a transposon insertion upstream of the tail domain (Patel et al., 1993), had  $6.4 \pm 0.25$  hyp7 nuclei in the dorsal cord (Fig. 2F,I;  $n=22$ ). *unc-116(rh24sb79)* is a recessive, partial loss-of-function allele with three amino acid changes in the motor domain, which leads to severely uncoordinated animals (Yang et al., 2005). These animals had a weak hyp7 nuclear migration defect with an average of  $0.8 \pm 0.17$  nuclei in the dorsal cord (Fig. 2G,I;  $n=57$ ). Some *unc-116(rh24sb79)* animals had as many as six nuclei in the dorsal cord. *unc-116(f122)* encodes a kinesin heavy chain truncated after the motor and neck regions (D. Thierry-Mieg, personal communication); this severe allele is lethal and is maintained using an UNC-116::GFP rescuing construct. This construct rescues the *unc-116* deficiency incompletely; transgenic animals have an average of  $2.4 \pm 0.68$  nuclei in the dorsal cord, with as many as nine nuclei seen in the dorsal cords of individual animals (Fig. 2H,I;  $n=19$ ). Thus, loss of function in *unc-116* results in defects in hyp7 nuclear migration.

Our previous model of nuclear migration in *C. elegans* proposed that UNC-83 and UNC-84 bridge the nuclear envelope and connect the cytoskeleton with the nuclear lamina. We now propose that UNC-83 is in the outer nuclear membrane with its N-terminal domain in the cytoplasm, where it interacts with KLC-2 to recruit kinesin to the surface of the nuclear envelope. Thus, kinesin-1 moves nuclei by connecting to the nuclear lamina through the UNC-83–UNC-84 bridge.

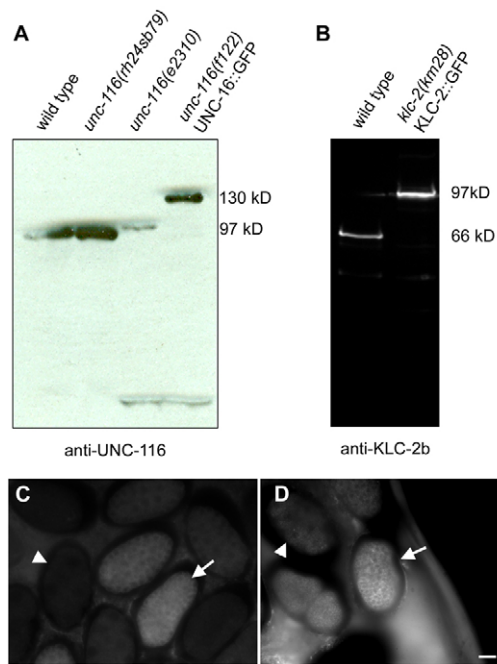


**Fig. 3. Specificity of the anti-KLC-2 and anti-UNC-116 antibodies.** (A) A western blot (developed on film) with anti-UNC-116 antibodies. A single band of ~97 kDa is detected in immunoblots of mixed-stage wild-type worms (lane 1) as well as *unc-116(rh24sb79)* (lane 2) and *unc-116(e2310)* (lane 3) animals. A single band of ~113 kDa in immunoblots of mixed-stage *unc-116(f122)*; UNC-116::GFP animals corresponds to the expected size of UNC-116::GFP (lane 4). (B) A western blot (imaged by digital camera) with anti-KLC-2 antibodies. Bands were detected of ~66 kDa in wild-type embryos (lane 1) and 97 kDa in *klc-2(km28)*; KLC-2::GFP embryos, corresponding to KLC-2::GFP (lane 2). (C,D) Wide-field fluorescence images of wild-type embryos stained with the anti-KLC-2 or UNC-116 antibodies. (C) KLC-2 expression is low in early embryos, such as in the 4-cell stage embryo shown (arrowhead). Expression increases greatly in the pre-elongation stage (arrow). (D) UNC-116 expression in early embryos is relatively low and diffuse, such as in the 8-cell embryo shown (arrowhead). Expression is much higher and more organized in the pre-elongation stage (arrow). Scale bar: 10  $\mu$ m.

### Localization of kinesin-1 in migrating hyp7 cells

Immunofluorescence was used to examine the expression of KLC-2 and UNC-116 in hyp7 cells at the time of nuclear migration. Antibodies against KLC-2 and UNC-116 had been previously raised in rabbits (Yang et al., 2005). The specificity of these antibodies was confirmed by western blot analysis (Fig. 3A,B). Affinity-purified anti-UNC-116 antibodies recognized a single polypeptide in immunoblots of mixed-stage wild-type, *unc-116(e2310)* and *unc-116(rh24sb79)* animals. In immunoblots of *unc-116(f122)*; UNC-116::GFP animals, the anti-UNC-116 antibodies recognized a single polypeptide corresponding to the UNC-116::GFP construct (Fig. 3A). Affinity-purified anti-KLC-2 antibodies recognized a single polypeptide in wild-type and *klc-2(km11)* mixed-stage animals (Fig. 3B). In *klc-2(km28)*; KLC-2::GFP animals, the antibodies only recognized a band corresponding to the size of the KLC-2::GFP construct (Fig. 3B), consistent with *klc-2(km28)* being a null allele.

Expression of both proteins, as observed in immunofluorescence assays, was low in the early embryo and increased markedly in hypodermal cells by the pre-coma stage, during which hyp7 nuclear migration takes place (Fig. 3C,D). Staining was absent in *klc-*

*2(km28)* and in *unc-116(f122)* embryos, consistent with the prediction that these are null or severe hypomorphic alleles and that the antibodies are specific (Fig. 4C,G). KLC-2 and UNC-116 expression in the hypomorphic *klc-2(km11)*, *unc-116(e2310)* and *unc-116(rh24sb79)* mutants was similar to in the wild type, although slightly decreased (Fig. 4B,E,F). In wild-type pre-comma embryos, KLC-2 and UNC-116 expression was seen in many cells, including hyp7 precursors at the time of nuclear migration, and was primarily cytoplasmic (Fig. 4A,D,H-K). Although the data were not conclusive, there might have been a slight enrichment of kinesin-1 at the nuclear envelope of migrating nuclei (Fig. 4H-K, arrows) as compared with other hypodermal nuclei (Fig. 4H-K, arrowheads).

The spatial and temporal expression of kinesin-1 is consistent with a role in hyp7 nuclear migration because KLC-2 and UNC-116 are expressed in the cytoplasm of hyp7 cells at the time of nuclear migration. Since kinesin-1 is likely to interact with many cargos in different locations in the cell, clear co-localization of UNC-83 and kinesin-1 at the nuclear envelope was not observed. This made it difficult to determine whether the KLC-2 and UNC-116 staining patterns were altered in *unc-83(e1408)* mutant embryos (data not shown). Nonetheless, the staining patterns are compatible with the hypothesis that a small pool of kinesin-1 co-localizes with UNC-83 at the nuclear envelope at the time of nuclear migration.

### UNC-83 recruits KLC-2 to the nuclear envelope in transfected mammalian tissue culture cells

Although our immunofluorescence data were consistent with the hypothesis that UNC-83 recruits kinesin-1 to the surface of migrating hyp7 nuclei, they failed to prove an UNC-83-dependent localization of kinesin-1 to the nuclear envelope. We therefore tested whether *C. elegans* UNC-83 could interact in vivo with *C. elegans* KLC-2 and recruit it to the nuclear envelope of mammalian tissue culture cells. It was previously shown that *C. elegans* UNC-83 localizes to the outer nuclear membrane in transiently transfected mammalian tissue culture cells (McGee et al., 2006). Here, the cytoplasmic domain of UNC-83c, with and without its transmembrane and KASH domains, was co-expressed with KLC-2 in HeLa cells. As expected, UNC-83 localized to the nuclear envelope in a KASH-dependent manner. Full-length UNC-83 recruited KLC-2 to the nuclear envelope (Fig. 5A,B), but UNC-83 $\Delta$ KASH failed to do so (Fig. 5C,D). These data suggest that UNC-83 recruits KLC-2 to the nuclear envelope in vivo.

### A KLC-2::KASH chimeric protein partially bypasses the requirement of UNC-83 for nuclear migration

The data from the above experiments suggest a model in which UNC-83 on the outer nuclear envelope functions as an adapter that links the nucleus to the microtubule cytoskeleton through kinesin-1. To test whether this is the primary function of UNC-83, we created a chimeric protein in which the transmembrane and KASH domains of UNC-83 were fused to the C-terminus of KLC-2. For tracking purposes, a 6-myc tag was engineered between the KLC-2 sequence and the transmembrane-KASH domain. Plasmid DNA encoding KLC-2::myc::KASH was injected into *unc-83(e1408)* animals to create two independent transgenic lines. Staining with anti-KLC-2 and anti-myc antibodies indicated that the KASH domain of UNC-83 efficiently targeted KLC-2 to the nuclear envelope (Fig. 6B,C). Staining with antibodies against UNC-116 indicated that overexpression of KLC-2 in the form of the KLC-2::myc::KASH construct did not alter UNC-116 localization (Fig. 6D,E). We hypothesize that a small, undetectable population of UNC-116

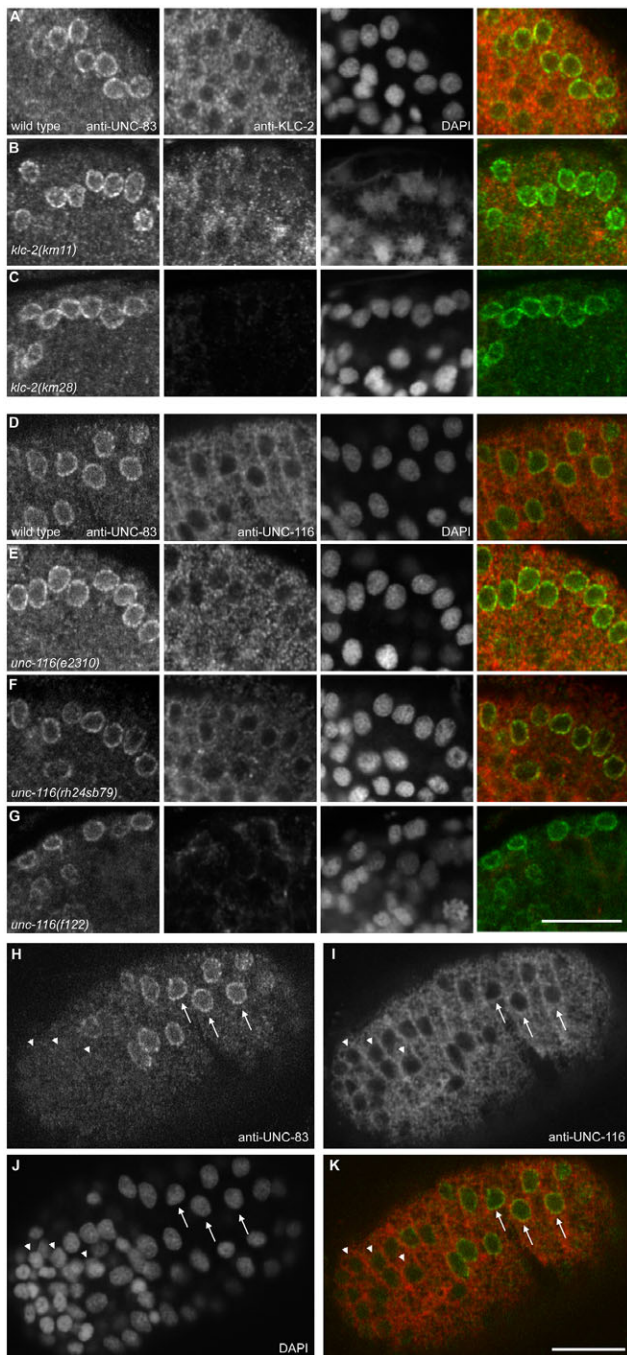


**Fig. 4. Kinesin-1 is expressed in hyp7 cells during nuclear migration.** (A-G) Single-slice confocal images of dorsal views of pre-elongation *C. elegans* embryos undergoing hyp7 nuclear migration. Immunolocalization of UNC-83 is shown in the left-most column, KLC-2 (A-C) or UNC-116 (D-G) in the second column, followed by DAPI staining of DNA in the third column, and a merge of UNC-83 (green) and KLC-2 or UNC-116 (red) localization in the right-most column. (A-C) KLC-2 localization in (A) wild-type, (B) *klc-2(km11)* and (C) *klc-2(km28)* embryos. (D-G) UNC-116 localization in (D) wild-type, (E) *unc-116(e2310)*, (F) *unc-116(rh24sb79)* and (G) *unc-116(f122)* embryos. (H-K) A single-slice confocal image of a dorsal view of the pre-elongation wild-type embryo shown in D. (H) UNC-83 immunostaining (green in merge); (I) UNC-116 immunostaining (red in merge); (J) DAPI staining of DNA; (K) merge of H and I. Arrows indicate UNC-83-positive hyp7 nuclei and arrowheads mark other hypodermal nuclei. In all images, anterior is to the left. Scale bars: 10  $\mu$ m.

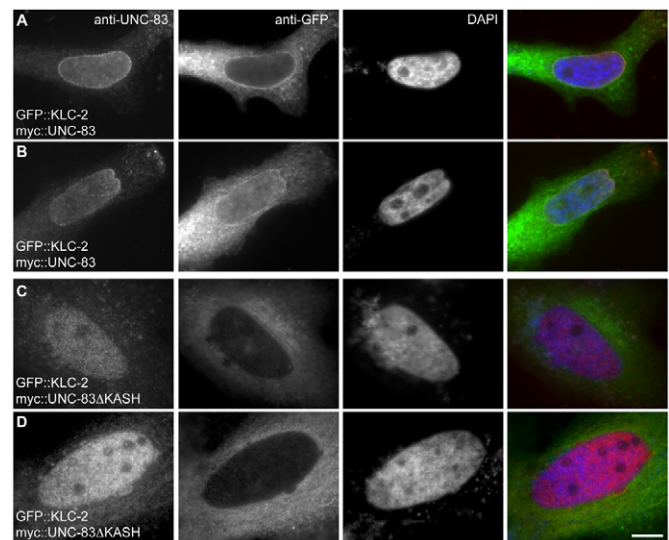


**Fig. 5. UNC-83 recruits kinesin-1 to the nuclear envelope.** HeLa cells transiently transfected with DNA encoding GFP::KLC-2 and (A,B) full-length myc::UNC-83 or (C,D) myc::UNC-83 $\Delta$ KASH. Shown are immunolocalization of UNC-83 (column 1) or KLC-2 (column 2), DAPI staining of DNA (column 3) and a merge of UNC-83 (red), KLC-2 (green) and DAPI (blue) staining (column 4). UNC-83 can be seen enriched at the nuclear envelope with KLC-2. UNC-83 $\Delta$ KASH is partially imported into the nucleus and, in this case, KLC-2 remains cytoplasmic. Scale bar: 10  $\mu$ m.

was recruited to the nuclear envelope, while most of the limited pool of UNC-116 was engaged in nuclear-independent roles elsewhere in the cell. To test the function of the chimeric protein in nuclear migration, we counted hyp7 nuclei in the dorsal cords of transgenic animals. The two transgenic lines had averages of  $7.45 \pm 0.51$  and  $5.67 \pm 0.62$  nuclei in the dorsal cord ( $n=20$ ), significantly lower than the *unc-83(e1408)* null mutant phenotype of  $11.8 \pm 0.14$  nuclei (Fig. 6A). Thus, the KLC-2::KASH chimeric protein can partially rescue the *unc-83* null phenotype. Although not complete, this level of rescue was similar to that reported for some lines of *unc-83(e1408)* rescued with a wild-type *unc-83* construct (McGee et al., 2006).

## DISCUSSION

In this study, we present genetic data that show the requirement for both subunits of kinesin-1, i.e. UNC-116 and KLC-2, during *C. elegans* hyp7 nuclear migration (Fig. 2). Furthermore, we demonstrate a direct interaction between the N-terminal region of KLC-2 and a portion of the cytoplasmic domain of UNC-83 (Figs 1 and 5). Together, these data suggest that UNC-83 is the nuclear-specific cargo adaptor for kinesin-1 (Fig. 7A). To test this role for UNC-83, KLC-2 was artificially targeted to the outer nuclear membrane in the absence of UNC-83 by fusing a KASH domain to KLC-2. The KLC-2::KASH hybrid protein was able to partially bypass the requirement of UNC-83 for hyp7 nuclear migration (Fig. 6). We therefore conclude that UNC-83 functions primarily as a docking site at the cytoplasmic surface of the nuclear envelope to recruit the plus-end-directed microtubule motor kinesin-1, which in turn generates the major force to move nuclei. Unpublished data from our laboratory suggest that the non-kinesin-interacting domain of the cytoplasmic portion of UNC-83 interacts with several proteins that are likely to function to regulate kinesin and nuclear migration.

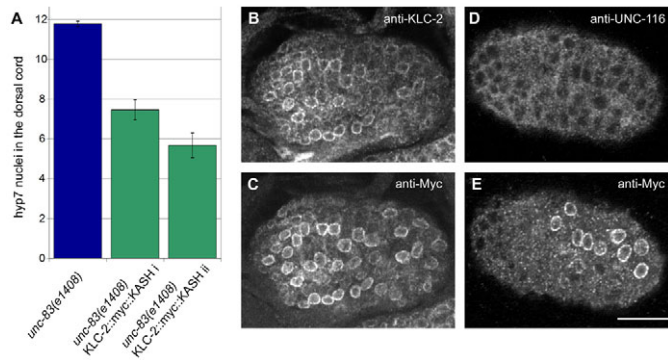


**Fig. 6. The KLC-2::KASH construct can partially bypass the requirement of UNC-83 for hyp7 nuclear migration.**

(A) The average number of hyp7 nuclei counted in the dorsal cord of *unc-83(e1408)* null animals ( $n=71$ ) and two lines of *unc-83(e1408); ycEx117,118[pSL440(KLC-2::myc::KASH)]* (KLC-2::myc::KASH i, ii) ( $n=20$ ). Error bars indicate s.e. (B-E) Single-slice confocal images of pre-elongation embryos. (B) An *unc-83(e1408); ycEx118[pSL440(KLC-2::myc::KASH)]* (KLC-2::myc::KASH i) embryo stained with the anti-KLC-2 antibody. (C) The same embryo and focal plane as in B, stained with an anti-myc antibody. (D) An *unc-83(e1408); ycEx118[pSL440(KLC-2::myc::KASH)]* (KLC-2::myc::KASH ii) embryo stained with the anti-UNC-116 antibody. (E) The same embryo and focal plane as in D, stained with an anti-myc antibody. Dorsal views with anterior on the left. Scale bar: 10 μm.

### A model for *C. elegans* nuclear migration

Our model of nuclear migration in *C. elegans* proposes that UNC-84 and UNC-83 bridge the nuclear envelope and connect the cytoskeleton with the nuclear lamina (Fig. 7A) (Lee et al., 2002; McGee et al., 2006; Starr, 2007; Starr et al., 2001). In this model, dimers or multimers of UNC-84 localize to the inner nuclear membrane, where their N-termini interact with the nuclear lamina while their C-terminal SUN domains extend into the perinuclear space. The SUN and linker domains of UNC-84 then recruit UNC-83 to the outer nuclear membrane through a direct interaction with the KASH domain of UNC-83 (McGee et al., 2006). This positions UNC-83 in the outer nuclear membrane with its N-terminal domain extending into the cytoplasm (Fig. 7A). The interaction between UNC-83 and KLC-2 implies that the role of UNC-83 during nuclear migration is to recruit kinesin-1 to the nuclear envelope. The KLC-2 and UNC-116 immunostaining patterns were compatible with the hypothesis that a small pool of kinesin-1 co-localizes with UNC-83 at the nuclear envelope at the time of nuclear migration. Moreover, when expressed in HeLa cells, UNC-83 recruited KLC-2 to the nuclear envelope (Fig. 5). Most significantly for our model, analysis of *klc-2* and *unc-116* mutant lines showed that loss-of-function mutations in either component of kinesin-1 result in a severe hyp7 nuclear migration defect. Thus, the UNC-83–KLC-2 interaction is functionally required for nuclear migration in hyp7 cells. Based on these findings, we conclude that kinesin-1 is the primary motor responsible for the translocation of the nucleus along microtubules.

### Organization of the microtubule cytoskeleton during nuclear migration

Microtubules are required for hyp7 nuclear migration, as treatment of embryos with nocodazole results in complete failure of hyp7 nuclear migration (Williams-Masson et al., 1998). Kinesin-1 is a plus-end-directed microtubule motor. Thus, if kinesin-1 provides the force for nuclear migration, the

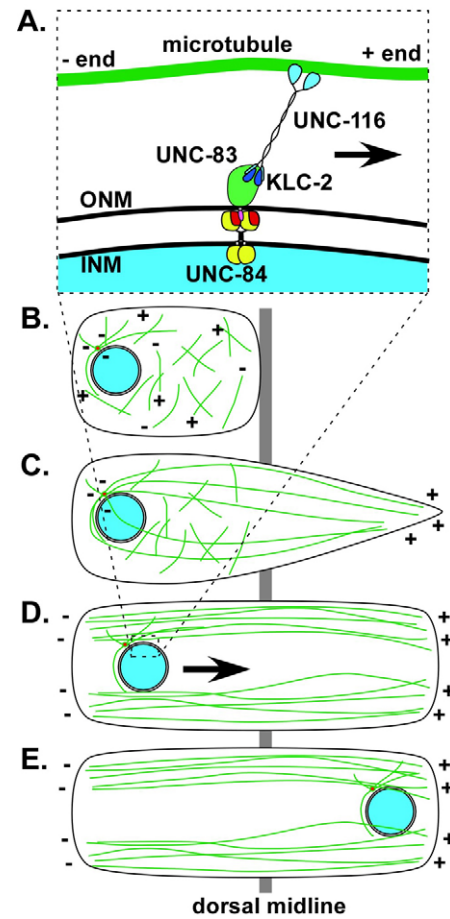


**Fig. 7. A model of nuclear migration in *C. elegans* hyp7 cells.**

(A) The nuclear envelope during nuclear migration. UNC-84 (red and yellow) localizes to the inner nuclear membrane (INM) and UNC-83 (green and pink) localizes to the outer nuclear membrane (ONM). The UNC-84 SUN domain (red) interacts with the UNC-83 KASH domain (pink) in the perinuclear space. The cytoplasmic domain of UNC-83 (green) interacts with KLC-2 (dark blue). The motor activity of UNC-116 (light blue) moves hyp7 nuclei toward the plus ends of polarized microtubules (green). (B) Microtubules (green) resemble a meshwork at the beginning of cell intercalation (plus and minus ends of microtubules marked). (C) As intercalation proceeds across the dorsal midline (gray), microtubules nucleated from the centrosome (red) at the stationary end of the cell (left) extend into the growing tip (right) of the cell. (D) At the completion of intercalation, most microtubules are arranged in polarized, centrosome-independent bundles parallel to the cell boundaries. (E) Nuclei (blue) move along these polarized microtubule bundles (in the direction of the arrow in D).

microtubules in the cell must be polarized with their plus ends away from the nucleus. The organization of the microtubule cytoskeleton during hyp7 intercalation has been described in a series of fixed images (Williams-Masson et al., 1998). At the beginning of cell intercalation, microtubules resemble a meshwork (Fig. 7B). By the time the cells have completed intercalation, microtubules form long, thick bundles that align parallel to the long axis of the cell in the direction of nuclear migration (Fig. 7C,D). Williams-Masson et al. (Williams-Masson et al., 1998) propose a model in which microtubules are nucleated at the stationary end of each cell, where the nuclei are initially positioned, and extend in a polarized fashion with their plus ends

toward the intercalating tip of the cell (Fig. 7C). This would allow for a parallel array of microtubules to form in the correct orientation for plus-end-directed nuclear migration (Fig. 7D). During nuclear migration, parallel arrays of microtubules are likely to be independent of centrosomes because the centrosome moves with the nucleus. This would require a different mechanism from nuclear migrations that are pulled forward by centrosomes positioned in front, such as pronuclear migration and nuclear migration in a neurite (Meyerzon et al., 2009; Tsai et al., 2007). Previous data from our laboratory show that centrosomes remain attached to migrating hyp7 nuclei, but are not polarized in the direction of migration (Lee et al., 2002; Starr et al., 2001). If the hyp7 microtubules behave as proposed in this model, kinesin-1 could then transport the nuclei in the observed pattern, from the stationary end of the cell towards the plus ends of stabilized microtubule bundles that are extended into the new tip of the intercalating cell.

### The role of kinesin and KASH proteins in nuclear migration in other systems

The mechanism of targeting kinesin-1 to the outer nuclear envelope through an interaction with a KASH protein is likely to be conserved in other systems. KASH proteins have been identified across eukaryotes from yeast to mammals. In general, their N-terminal cytoplasmic domains are divergent and function in a variety of cellular and developmental events, including centrosome attachment to the nucleus, nuclear migration and tethering nuclei to the actin cytoskeleton (Starr and Fischer, 2005). Previously, other KASH proteins have been implicated in kinesin regulation. Mammalian SYNE1 (also known as nesprin 1 and a homolog of *C. elegans* ANC-1) interacts with kinesin-2 subunit KIF3B at the midbody, where they function during cytokinesis (Fan and Beck, 2004). It is unknown whether SYNE1 also recruits kinesin-2 to the nuclear envelope during nuclear migration.

Recent evidence suggests that the mechanism described here for UNC-83 to recruit kinesin-1 to the nuclear envelope is conserved in flies and mammals. Although no clear homologs of UNC-83 have been identified outside of nematodes, we propose that the mammalian nesprin 4 and *Drosophila klarsicht* (*klar*) genes are homologs of UNC-83. *Drosophila klar* encodes a KASH protein that is not obviously conserved outside of insects and is required for nuclear migration in the developing eye neuroepithelium (Patterson et al., 2004). Although no direct interaction has been reported, KLAR is thought to function through kinesin-1 to mediate the movement of nuclei and lipid droplets (Shubeita et al., 2008; Welte et al., 1998). Mammalian nesprin 4 is a newly identified KASH protein with no obvious homologs outside of vertebrates (Roux et al., 2009). No loss-of-function phenotype has been reported for nesprin 4. However, like UNC-83, nesprin 4 interacts with kinesin-1 through the light chain and recruits kinesin-1 to the nuclear envelope when expressed in heterologous HeLa cells (Roux et al., 2009). Based on the above reasoning, we hypothesize that nesprin 4 in humans and KLAR in *Drosophila* function in a homologous manner to UNC-83 in *C. elegans* to coordinate kinesin-1 at the nuclear envelope during nuclear migration.

### Acknowledgements

We thank Dmitry Kolesnikov for technical help and Leslee Rose, Guangshuo Oh and members of the Starr and McNally laboratories for helpful comments. This research was supported by grants R01GM073874 to D.A.S. and R01GM079421 to F.J.M. from the National Institutes of Health. Deposited in PMC for release after 12 months.

### References

- Bowman, A. B., Kamal, A., Ritchings, B. W., Philp, A. V., McGrail, M., Gindhart, J. G. and Goldstein, L. S. (2000). Kinesin-dependent axonal transport is mediated by the Sunday driver (SYD) protein. *Cell* **103**, 583-594.
- Fan, J. and Beck, K. A. (2004). A role for the spectrin superfamily member Syne-1 and kinesin II in cytokinesis. *J. Cell Sci.* **117**, 619-629.
- Gindhart, J. G. (2006). Towards an understanding of kinesin-1 dependent transport pathways through the study of protein-protein interactions. *Brief. Funct. Genomic. Proteomic.* **5**, 74-86.
- Glater, E. E., Megeath, L. J., Stowers, R. S. and Schwarz, T. L. (2006). Axonal transport of mitochondria requires Milton to recruit kinesin heavy chain and is light chain independent. *J. Cell Biol.* **173**, 545-557.
- Guo, Y., Jangi, S. and Welte, M. A. (2005). Organelle-specific control of intracellular transport: distinctly targeted isoforms of the regulator Klar. *Mol. Biol. Cell* **16**, 1406-1416.
- Horvitz, H. R. and Sulston, J. E. (1980). Isolation and genetic characterization of cell-lineage mutants of the nematode *Caenorhabditis elegans*. *Genetics* **96**, 435-454.
- Karcher, R. L., Deacon, S. W. and Gelfand, V. I. (2002). Motor-cargo interactions: the key to transport specificity. *Trends Cell Biol.* **12**, 21-27.
- Konecna, A., Frischknecht, R., Kinter, J., Ludwig, A., Steuble, M., Meskenaitė, V., Indermuhle, M., Engel, M., Cen, C., Mateos, J. M. et al. (2006). Calsyntenin-1 docks vesicular cargo to kinesin-1. *Mol. Biol. Cell* **17**, 3651-3663.
- Lee, K. K., Starr, D., Cohen, M., Liu, J., Han, M., Wilson, K. L. and Gruenbaum, Y. (2002). Lamin-dependent localization of UNC-84, a protein required for nuclear migration in *Caenorhabditis elegans*. *Mol. Biol. Cell* **13**, 892-901.
- Malone, C. J., Fixsen, W. D., Horvitz, H. R. and Han, M. (1999). UNC-84 localizes to the nuclear envelope and is required for nuclear migration and anchoring during *C. elegans* development. *Development* **126**, 3171-3181.
- McGee, M. D., Rillo, R., Anderson, A. S. and Starr, D. A. (2006). UNC-83 is a KASH protein required for nuclear migration and is recruited to the outer nuclear membrane by a physical interaction with the SUN protein UNC-84. *Mol. Biol. Cell* **17**, 1790-1801.
- Meyerzon, M., Gao, Z., Liu, J., Wu, J.-C., Malone, C. J. and Starr, D. A. (2009). Centrosome attachment to the *C. elegans* male pronucleus is dependent on the surface area of the nuclear envelope. *Dev. Biol.* **327**, 433-446.
- Ong, L. L., Lim, A. P., Er, C. P., Kuznetsov, S. A. and Yu, H. (2000). Kinectin-kinesin binding domains and their effects on organelle motility. *J. Biol. Chem.* **275**, 32854-32860.
- Patel, N., Thierry-Mieg, D. and Mancillas, J. R. (1993). Cloning by insertional mutagenesis of a cDNA encoding *Caenorhabditis elegans* kinesin heavy chain. *Proc. Natl. Acad. Sci. USA* **90**, 9181-9185.
- Patterson, K., Molofsky, A. B., Robinson, C., Acosta, S., Cater, C. and Fischer, J. A. (2004). The functions of Klarsicht and nuclear lamin in developmentally regulated nuclear migrations of photoreceptor cells in the *Drosophila* eye. *Mol. Biol. Cell* **15**, 600-610.
- Roux, K. J., Crisp, M. L., Liu, Q., Kim, D., Kozlov, S., Stewart, C. L. and Burke, B. (2009). Nesprin 4 is an outer nuclear membrane protein that can induce kinesin-mediated cell polarization. *Proc. Natl. Acad. Sci. USA* **106**, 2194-2199.
- Rupp, R. A., Snider, L. and Weintraub, H. (1994). *Xenopus* embryos regulate the nuclear localization of XMyoD. *Genes Dev.* **8**, 1311-1323.
- Sagasti, A., Hisamoto, N., Hyodo, J., Tanaka-Hino, M., Matsumoto, K. and Bargmann, C. I. (2001). The CaMKII UNC-43 activates the MAPKKK NSY-1 to execute a lateral signaling decision required for asymmetric olfactory neuron fates. *Cell* **105**, 221-232.
- Sakamoto, R., Byrd, D. T., Brown, H. M., Hisamoto, N., Matsumoto, K. and Jin, Y. (2005). The *Caenorhabditis elegans* UNC-14 RUN domain protein binds to the kinesin-1 and UNC-16 complex and regulates synaptic vesicle localization. *Mol. Biol. Cell* **16**, 483-496.
- Shubeita, G. T., Tran, S. L., Xu, J., Vershinin, M., Cermelli, S., Cotton, S. L., Welte, M. A. and Gross, S. P. (2008). Consequences of motor copy number on the intracellular transport of kinesin-1-driven lipid droplets. *Cell* **135**, 1098-1107.
- Starr, D. A. (2007). Communication between the cytoskeleton and the nuclear envelope to position the nucleus. *Mol. Biosyst.* **3**, 583-589.
- Starr, D. A. and Fischer, J. A. (2005). KASH 'n Karry: the KASH domain family of cargo-specific cytoskeletal adaptor proteins. *BioEssays* **27**, 1136-1146.
- Starr, D. A., Hermann, G. J., Malone, C. J., Fixsen, W., Priess, J. R., Horvitz, H. R. and Han, M. (2001). unc-83 encodes a novel component of the nuclear envelope and is essential for proper nuclear migration. *Development* **128**, 5039-5050.
- Sulston, J. E. (1983). Neuronal cell lineages in the nematode *Caenorhabditis elegans*. *Cold Spring Harb. Symp. Quant. Biol.* **48**, 443-452.
- Sulston, J. E. and Horvitz, H. R. (1981). Abnormal cell lineages in mutants of the nematode *Caenorhabditis elegans*. *Dev. Biol.* **82**, 41-55.
- Toyoshima, I., Yu, H., Steuer, E. R. and Sheetz, M. P. (1992). Kinectin, a major kinesin-binding protein on ER. *J. Cell Biol.* **118**, 1121-1131.

- Tsai, J. W., Bremner, K. H. and Vallee, R. B.** (2007). Dual subcellular roles for LIS1 and dynein in radial neuronal migration in live brain tissue. *Nat. Neurosci.* **10**, 970-979.
- Tsuboi, D., Hikita, T., Qadota, H., Amano, M. and Kaibuchi, K.** (2005). Regulatory machinery of UNC-33/Ce-CRMP localization in neurites during neuronal development in *Caenorhabditis elegans*. *J. Neurochem.* **95**, 1629-1641.
- Vale, R. D., Reese, T. S. and Sheetz, M. P.** (1985). Identification of a novel force-generating protein, kinesin, involved in microtubule-based motility. *Cell* **42**, 39-50.
- Verhey, K. J., Meyer, D., Deehan, R., Blenis, J., Schnapp, B. J., Rapoport, T. A. and Margolis, B.** (2001). Cargo of kinesin identified as JIP scaffolding proteins and associated signaling molecules. *J. Cell Biol.* **152**, 959-970.
- Weaver, C., Farr, G. H., 3rd, Pan, W., Rowning, B. A., Wang, J., Mao, J., Wu, D., Li, L., Larabell, C. A. and Kimelman, D.** (2003). GBP binds kinesin light chain and translocates during cortical rotation in *Xenopus* eggs. *Development* **130**, 5425-5436.
- Welte, M. A., Gross, S. P., Postner, M., Block, S. M. and Wieschaus, E. F.** (1998). Developmental regulation of vesicle transport in *Drosophila* embryos: forces and kinetics. *Cell* **92**, 547-557.
- Williams-Masson, E. M., Heid, P. J., Lavin, C. A. and Hardin, J.** (1998). The cellular mechanism of epithelial rearrangement during morphogenesis of the *Caenorhabditis elegans* dorsal hypodermis. *Dev. Biol.* **204**, 263-276.
- Yang, H. Y., Mains, P. E. and McNally, F. J.** (2005). Kinesin-1 mediates translocation of the meiotic spindle to the oocyte cortex through KCA-1, a novel cargo adapter. *J. Cell Biol.* **169**, 447-457.
- Yang, Z., Hong, S. H. and Privalsky, M. L.** (1999). Transcriptional anti-repression. Thyroid hormone receptor beta-2 recruits SMRT corepressor but interferes with subsequent assembly of a functional corepressor complex. *J. Biol. Chem.* **274**, 37131-37138.
- Yochem, J., Gu, T. and Han, M.** (1998). A new marker for mosaic analysis in *Caenorhabditis elegans* indicates a fusion between hyp6 and hyp7, two major components of the hypodermis. *Genetics* **149**, 1323-1334.